NANO EXPRESS

Open Access

CrossMark

Hysteresis of Low-Temperature Thermal Conductivity and Boson Peak in Glassy (g) As$_2$S$_3$: Nanocluster Contribution

V. Mitsa[1*], A. Feher[2], S. Petretskyi[1], R. Holomb[1], V. Tkac[2,3], P. Ihnatolia[1] and A. Laver[1]

Abstract

Experimental results of the thermal conductivity ($k(T)$) of nanostructured g-As$_2$S$_3$ during cooling and heating processes within the temperature range from 2.5 to 100 K have been analysed. The paper has considered thermal conductivity is weakly temperature $k(T)$ dependent from 2.5 to 100 K showing a plateau in region from 3.6 to 10. 7 K during both cooling and heating regimes. This paper is the first attempt to consider the $k(T)$ hysteresis above plateau while heating in the range of temperature from 11 to 60 K. The results obtained have not been reported yet in the scientific literature. Differential curve $\Delta k(T)$ of $k(T)$ (heating $k(T)$ curve minus cooling $k(T)$ curve) possesses a complex asymmetric peak in the energy range from 1 to 10 meV. $\Delta k(T)$ reproduces the density of states in a $g(\omega)/\omega^2$ representation estimated from a boson peak experimentally obtained by Raman measurement within the range of low and room temperatures. Theoretical and experimental spectroscopic studies have confirmed a glassy structure of g-As$_2$S$_3$ in cluster approximation. The origin of the low-frequency excitations resulted from a rich variety of vibrational properties. The nanocluster vibrations can be created by disorder on atomic scale.

Keywords: Chalcogenide glass, Thermal conductivity, Low temperatures, Nanostructured semiconductors, Boson peak, Raman spectroscopy

PACS: 61.43.Fs, 61.43.Bn, 31.15.A-, 63.50.Lm, 44.10. + i, 65.60. + a

Background

Chalcogenide glass (g) g-As$_2$S$_3$ is a canonical infrared optical material for practical applications in chalcogenide photonics. Thermal conductivity (k) is a property determining the working temperature levels of optical media during high-power infrared (IR) laser illumination [1]. Experimental discoveries of the low-temperature thermal anomalies of glasses have been first described in oxide glasses [2]. A few years later, anomaly at $T < 1$ K that was fixed with almost quadratic temperature dependence of thermal conductivity k was confirmed for g-As$_2$S$_3$ [3]. The anomaly at intermediate temperatures that range up to 10 K for g-As$_2$S$_3$ was discovered later [4]. Within this temperature range, the thermal conductivity exhibits a ubiquitous plateau [2, 3]. The glassy materials deviate from well-known universal thermal

properties at low temperatures for crystalline solids [2]. The experimental findings of thermal conductivity measurements on glasses below 1 K have been interpreted by most successful model [5, 6] in the terms of "two-level" or "tunnelling" systems, which were later named as "standard tunnelling model" (STM) [7, 8]. Within the frame of STM model, it has been assumed that the "plateau" behaviour arises from the existence of quasi-localized low-frequency (LF) modes [9]. Many models have been proposed for further description of the structural origin of the LF modes [10–22]. A number of them are related to the nanoheterogeneous nature of glasses. Nanoheterogeneities generate an intermediate range ordering in the chalcogenide glasses. This relates to an excess in vibrational density of states' contribution which is directly connected with the so-called boson peak (BP) observed by neutron or vibrational Raman spectroscopy [10, 11, 14, 18, 20, 21]. The theoretical explanation of the temperature dependence of the thermal conductivity

* Correspondence: v.mitsa@gmail.com
[1]Uzhhorod National University, Pidhirna Str., 46, Uzhhorod 88000, Ukraine
Full list of author information is available at the end of the article

Mitsa *et al. Nanoscale Research Letters* (2017) 12:345

Page 2 of 6

coefficient for glasses in the temperature range above the plateau has been considered on the basis of intermediate range ordering [18]. Theoretical and experimental spectroscopic studies confirm a glassy structure of g-As$_2$S$_3$ in cluster approximation. The origin of the low-frequency excitations resulted from a rich variety of vibrational properties of nanocluster vibrations [20, 21, 23, 24].

The aim of this work is to analyse the dependencies of low-frequency modes from system cluster size. Our efforts have been focused on the LF vibrational modes which may be involved in the measured BP and thermal conductivity in g-As$_2$S$_3$. The experiment has been carried out to study thermal conductivity behaviour during cooling and heating within the temperature range from 2.5 to 100 K.

Methods

The sample of optical quality was prepared by melting additionally purified elements of arsenic and sulphur in clean evacuated and sealed quartz ampoules placed at a rocking furnace at 600 °C for a period of 24 h. Then, it was cooled in the air with a cooling rate of 1 K/s. Such conditions of preparation minimized nanosize realgar cluster separation [25].

Thermal conductivity of the nanostructured g-As$_2$S$_3$ was studied between 2.5 and 100 K, during both cooling and heating procedures. The measurement was performed in commercial Quantum Design Physical Property Measurement System (PPMS) with a thermal transport option (TTO). Two-probe lead configuration has been chosen, due to the fact that the sample has small thermal conductivity. Pill-shaped sample ($2.5 \times 5 \times 5$ mm^3) has been cut for these measurements. It was glued between two disk-shaped copper leads (hot and cold platforms) with GE Varnish glue. The heater and hot thermometer were attached against each other at the hot platform. The cold thermometer and thermal reservoir were mounted on cold platform in the same way as hot platform. Thermal conductivity of the sample is much smaller than the thermal conductivity of the leads. The heat power was applied from the heater mounted on the hot platform in order to create a user-specified temperature gradient between the two thermometers mounted on cold and hot platforms. For measuring the continuous measurement mode was selected. During cooling and heating procedures, the measurements are being taken continually and the adaptive software is adjusting the parameters (such as heater power) to optimize the measurements. In the first study cycle, $k(T)$ 100 to 2.5 K temperature was held at cooling the sample with rate 0.385 K/min. The second series of measurements included both cooling with the rate of 0.385 K/min from 100 to 2.5 K temperature and heating with the rate of 0.415 K/min in the opposite direction. Based on thermal transport hardware and software, it was

possible to calculate thermal conductivity directly from the applied heater power, resulting ΔT, and sample geometry using the equation:

$$k = \frac{Pl}{S(T_2 - T_1)} \tag{1}$$

where k is the thermal conductivity (W/Km), P is applied heater power (W), l is the height of measured sample (m) and S is the cross sectional area of sample (m^2).
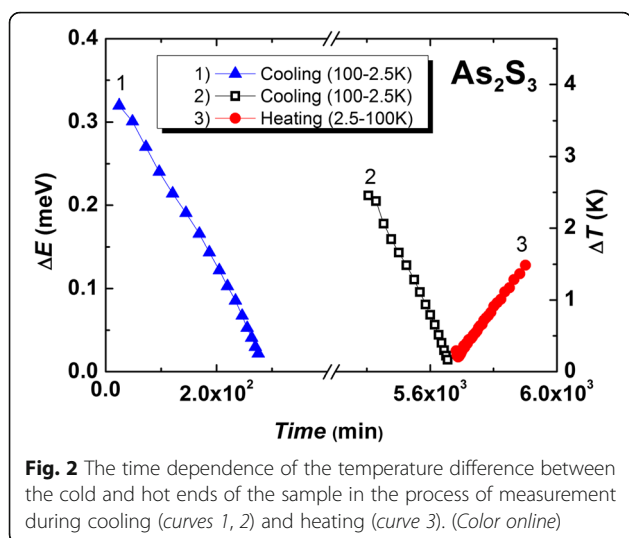
The results were obtained when experimental conditions have been selected to obtain maximum temperature uniformity across the sample. Depending on the time, the heater temperature and resulting ΔT have demonstrated linear trend for both series of measurements (Figs. 1 and 2). The accuracy of the measurement is equivalent to 3%. This paper focuses on the results taken from 2.5 to 100 K.

Room-temperature low-frequency Raman spectra were measured using a triple grating Dilor-XY800 spectrometer equipped with a CCD detector cooled by liquid nitrogen. The slit width was set to 1 cm^{-1}. Laser line of 632.8 nm was used as the excitation source.

Finite size atomic As$_n$S$_m$ nanoclusters containing structural units are expected to be important for glassy As-S system. For better modelling of the chemical environment, the dangling bonds of clusters were terminated by H atoms. These assumptions were used for the Raman study of active LF modes (Fig. 3). Density functional theory (DFT) calculations of optimal geometry, total and formation energies and electronic and vibrational properties of these clusters were performed, using GAMESS (US) program [26]. The pure corrected exchange functional proposed by Becke (B) [27] and the gradient-corrected correlation functional proposed by Lee, Yang and Parr (LYP) [28] were applied for calculations. The modified Stuttgart RLC ECP basis set [29] was
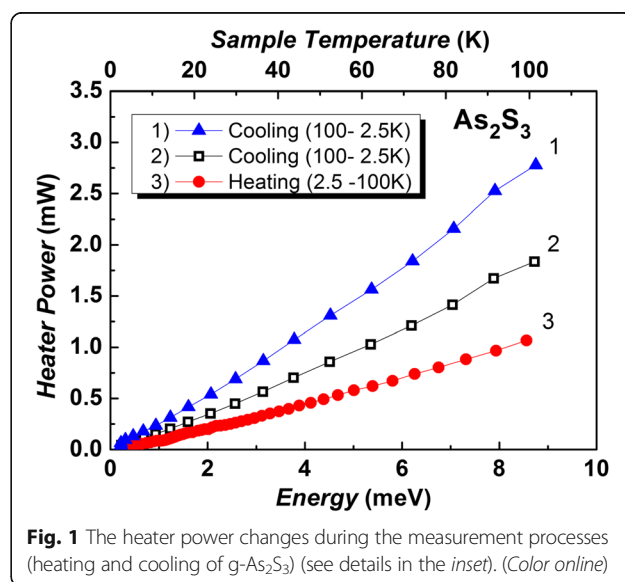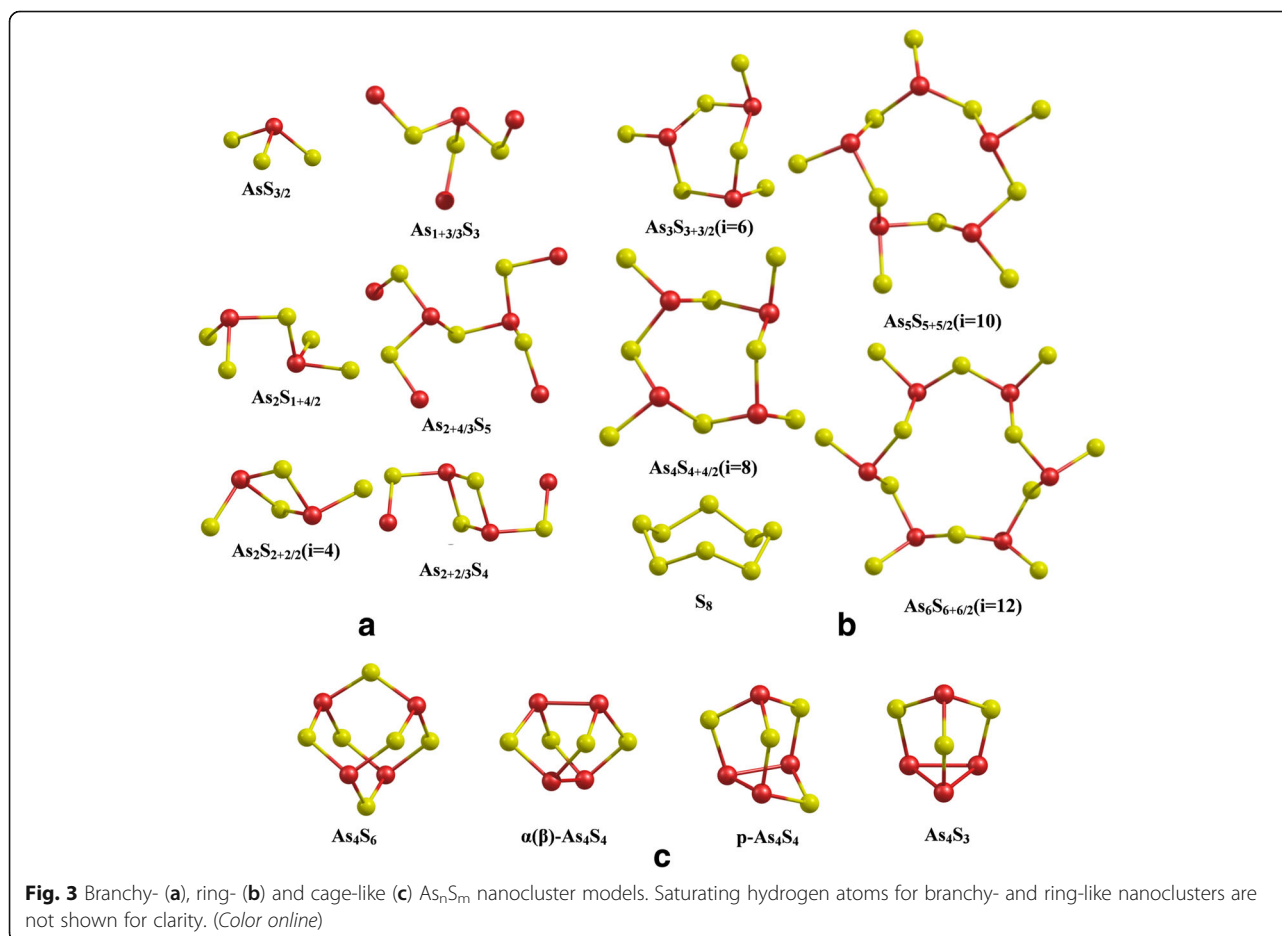

Fig. 1 The heater power changes during the measurement processes (heating and cooling of g-As$_2$S$_3$) (see details in the *inset*). (*Color online*)

Fig. 2 The time dependence of the temperature difference between the cold and hot ends of the sample in the process of measurement during cooling (curves 1, 2) and heating (curve 3). (*Color online*)
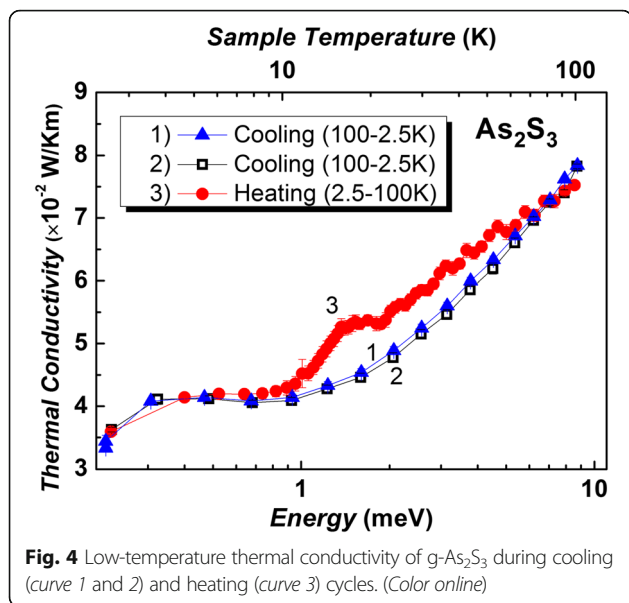
used for As and S atoms. The contribution of terminal H atoms' vibrations in the calculated Raman spectra of As_nS_m nanoclusters were subsequently eliminated. The details of basis set modification and spectral treatment have been already described [20, 21, 24].

Results and Discussion

The structural origin of low-temperature thermal conductivity and boson peak are still open for discussion and are the matter of debate [10–22]. The thermal conductivity in g-As_2S_3 studied between 2.5 and 100 K during cooling and heating procedure is shown at Fig. 4. The measured values of thermal conductivity agree with the data for chalcogenide glasses described earlier [15]. As it can be seen, the thermal conductivity $k(T)$ is slightly temperature dependent from 2.5 to 10 K showing a plateau region during both cooling and heating regimes (see Fig. 4). For temperature range mentioned above, the similar plateau in g-As_2S_3 has been found before [4]. The linear relationship with a $tg(\alpha) = 0.0003$ slope was found for the temperature dependencies $k(T)$ above the plateau (11–100 K) independently on different cooling cycles within the accuracy of measurement. At the same time, the jump in $k(T)$ dependence between cooling and heating cycles of g-As_2S_3 has been discovered (see Fig. 4). The values show that the jump of $k(T)$ during heating is greater than the accuracy of the measurement producing an appreciable deviation from $k(T)$ values taken during the cooling. The appearance of

Fig. 3 Branchy- (**a**), ring- (**b**) and cage-like (**c**) As_nS_m nanocluster models. Saturating hydrogen atoms for branchy- and ring-like nanoclusters are not shown for clarity. (*Color online*)

Mitsa *et al. Nanoscale Research Letters* (2017) 12:345

Page 4 of 6

Fig. 4 Low-temperature thermal conductivity of g-As$_2$S$_3$ during cooling (*curve 1* and *2*) and heating (*curve 3*) cycles. (*Color online*)

hysteresis in $k(T)$ during heating was fixed in the temperature range from 11 to 60 K. The difference curve $\Delta k(T)$ of $k(T)$ (heating minus cooling) has a complex asymmetric peak when energy is between 1 and 10 meV (Fig. 5) and reproduces the experimental low-temperature boson peak (excess of the density of states based on the Debye prediction). The BP seen by Raman measurements is shown in Fig. 5 in scale $g(\omega)/\omega^2$ (curve 1, $T = 10$ K [11], curve 2, $T = 293$ K). The position of $g(\omega)/\omega^2$ maximum at 2.65 eV in the experimental neutron scattering measurements of g-As$_2$S$_3$ density of state $g(\omega)$ is indicated in Fig. 5 by arrow for the
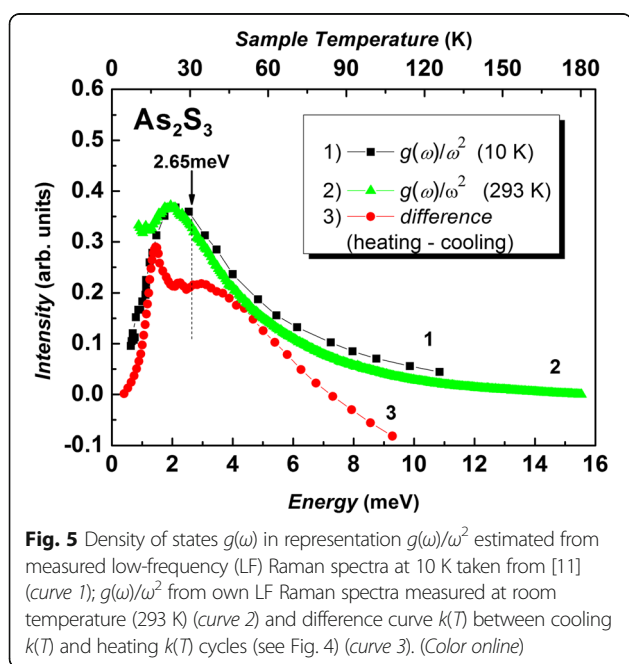
Fig. 5 Density of states $g(\omega)$ in representation $g(\omega)/\omega^2$ estimated from measured low-frequency (LF) Raman spectra at 10 K taken from [11] (*curve 1*); $g(\omega)/\omega^2$ from own LF Raman spectra measured at room temperature (293 K) (*curve 2*) and difference curve $k(T)$ between cooling $k(T)$ and heating $k(T)$ cycles (see Fig. 4) (*curve 3*). (*Color online*)

comparison. However, in addition to complex experimental investigations of $g(\omega)$ by neutron scattering [10], the position of maximum $g(\omega)/\omega^2$ mentioned above can be estimated by measuring the LF Raman spectra of glasses at 10 K (Fig. 5, curve 1) when contribution of quasi-elastic light scattering to the Raman spectra at below 10 cm^{-1} is negligible. According to theoretical calculations, the experimentally observed intensity (I_{exp}) in the low-frequency spectrum is given by [11]:

$$I_{exp}(\Delta\omega) = \frac{C(\Delta\omega)g(\Delta\omega)[n(\Delta\omega)+1]}{\Delta\omega}, \qquad (2)$$

where $C(\Delta\omega)$ is light-to-vibrations coupling coefficient, $\Delta\omega$ is a Raman shift and $g(\Delta\omega)$ is the density of state; $n(\Delta\omega) = \frac{1}{\exp\left(\frac{\hbar\Delta\omega}{kT}\right)-1}$ – Bose factor for the Stokes component.

Taking into account the mentioned above, the reduced intensity

$$I_{red}(\Delta\omega) = \frac{I_{exp}(\Delta\omega)}{\Delta\omega[n(\Delta\omega)+1]} = \frac{C(\Delta\omega)g(\Delta\omega)}{(\Delta\omega)^2}.$$

$$(3)$$

Based on neutron scattering measurements [10], the coupling coefficient $C(\Delta\omega)$ between the reduced Raman intensity (I_{red}) and the $g(\Delta\omega)$ is believed to be a monotonically increasing function $C(\Delta\omega) \approx \Delta\omega$ from 5–8 up to 100 cm^{-1}. In this case, the boson peak seen by Raman measurements is due to an anomaly in $g(\Delta\omega)$ and reflecting an enhancement of low-frequency states relative to an elastic continuum Debye level [11].

It is known that the BP in the low-frequency Raman spectra of glasses has also been related to the existence of intermediate range ordering (clusters) [18, 23, 24]. To understand how these low-frequency modes depend on the type and system size, several As-S clusters (namely branchy-, ring- and cage-like) were modelled (Fig. 3) and used to calculate the LF Raman active modes. It was found that among the clusters presented in Fig. 3, only the glass-network forming branchy- (a) and ring-like (b) clusters exhibit LF vibrational modes. No LF vibrational modes were found in the calculated Raman spectra of the rigid cage-like As-S nanoclusters (Fig. 3c).

Results have shown that a single pyramidal structural unit can be characterized by stretching and deformation type vibrations only, i.e. no LF modes were calculated for AsS$_{3/2}$ cluster. However, the further branching of this cluster leads to the appearance of LF vibrational modes in the calculated Raman spectra of As$_{1+3/3}$S$_3$ cluster at 23.5, 39.3 and 46.8 cm^{-1}. A correlation between LF modes and cluster size was also found when branching of As$_2$S$_{1+4/2}$ cluster takes place (see Fig. 3). For As$_2$S$_{1+4/2}$ cluster, LF Raman active modes were calculated at 31.7, 43.1 and 58.8 cm^{-1}. The

Mitsa *et al. Nanoscale Research Letters* (2017) 12:345

Page 5 of 6

number of LF vibrations of the branched structure (cluster $As_{2+4/3}S_5$) increases, and their frequencies shift towards low-frequency region: 12.8, 17.3, 23.5, 30.2, 32.8, 36.3 and 40.1 cm^{-1}. Similar situation can be found when calculated LF Raman active modes of $As_2S_{2+2/2}$ and $As_{2+2/3}S_4$ are compared. The LF Raman spectra simulated with Lorenz curves (full width at half maximum is 10 cm^{-1}) calculated for ring-like As-S nanoclusters are shown in Fig. 6. Both the frequency position and Raman intensity of the calculated bands of As-S rings show strong dependence on cluster size (i). As it can be seen, the most intensive band in the calculated LF Raman spectra of $As_3S_{3+3/2}$ cluster is located at ~56.1 cm^{-1}. With the increasing cluster size, the new Raman bands start to appear at lower frequency region of the simulated spectra (see Fig. 6). Two LF Raman bands centred at 19.7 and 53.4 cm^{-1} can clearly be seen in the simulated Raman spectra of 12-membered As-S ring (cluster $As_6S_{6+6/2}$).

The lowest vibrational mode of 6-, 8-, 10- and 12-membered rings (Fig. 3) is less intensive in the Raman spectra and is located at 33.1, 18.2, 10.8 and 9.0 cm^{-1}, respectively. The analysis of normal coordinates of these low-frequency vibrations indicate that they are torsional and out of plane bending vibrations involving group of
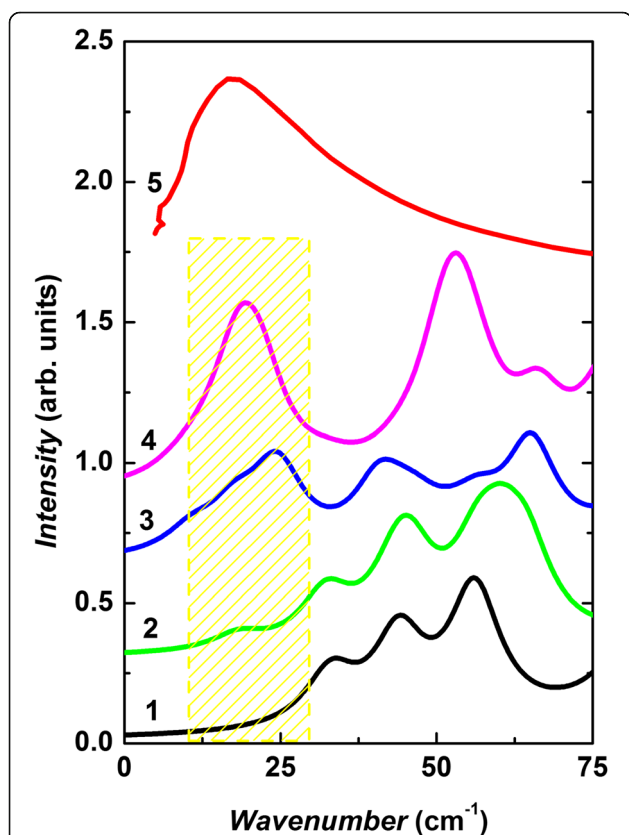
atoms (within 3–5 bonds). The atomic motions for some of these vibrations have a "wavelike" character. The larger *i*-member rings and branchy As_nS_m nanoclusters can be associated with the intermediate range order of As_2S_3 glass and produce the localized collective LF vibrations. This can be responsible for the low-temperature anomalies and BP of g-As_2S_3. Quasi-localized modes that resonantly couple with transverse phonons might lead to the accumulation of the low-energy modes around the boson peak [22].

It is important to note that with increasing the number of atoms in branched clusters $(As_2S_3)n$, $n = 1$–3, the energy formation decreases from −41.5 (cluster As_2S_3) to −124.6 Hartree (cluster As_6S_9). Lowering the formation energy of large clusters demonstrates the higher probability of such structure formation [30]. Calculated low-frequency vibrations of As_nS_m clusters demonstrate that the collective torsional and out of plane bending vibrations of the big 10- and 12-membered rings (10.8 and 9.0 cm^{-1}, respectively) and torsional vibrations of $As_{2+4/3}S_5$ branched A_nS_m clusters (12.8 cm^{-1}) can contribute to $g(\omega)/\omega^2$ (Fig. 6) and $k(T)$ above the plateau in g-As_2S_3 (Fig. 4).

Conclusions

The temperature dependence of the thermal conductivity $k(T)$ of g-As_2S_3 has been studied within the temperature range from 2.5 to 100 K during cooling and heating cycles. The presence of "plateau" in the $k(T)$ ranged from 3.6 to 10.7 K (0.31–0.92 meV) has been confirmed. Within the temperature range from 11 to 60 K, the hysteresis of temperature dependence during cooling and heating procedure has been observed above plateau. Dependencies $k(T)$ for different cooling cycles in the temperature range from 11 to 100 K, which is located above the plateau, within the accuracy of measurement have linear behaviour with a slope tg(α) = 0.0003. The contribution to thermal conductivity and boson peak in the Raman spectra can have torsion and out of plane bending vibrations of ring and branched clusters' origin.

Authors' Contributions
All authors (VM, AF, SP, RH, VT, PI and AL) equally contributed to developing the general idea and methodological aspects of the investigation. SP, AL and RH have prepared the source glasses and have synthesized As_2S_3 glasses. AF, SP and VT have performed the low-temperature thermal conductivity measurements to characterize the samples. RH, VM and PI performed the low-

Fig. 6 Simulated low-frequency Raman spectra of As_nS_m ring-like clusters (1–4): (1) $As_6S_{6+6/2}$, (2) $As_5S_{5+5/2}$, (3) $As_4S_{4+4/2}$, (4) $As_3S_{3+3/2}$ and $g(\omega)/\omega^2$ (10 K, ref. [11]) of g-As_2S_3 (5). (*Color online*)

Mitsa *et al. Nanoscale Research Letters* (2017) 12:345

Page 6 of 6

frequency Raman spectroscopy measurements, quantum-mechanical calculation of vibrational spectra of clusters and spectral interpretation. VM carried out the general control of the processing and analysis of the results. All authors proofread the final manuscript of the paper.

Competing Interests

The authors declare that they have no competing interests.

Publisher's Note

Springer Nature remains neutral with regard to jurisdictional claims in published maps and institutional affiliations.

Author details

[1]Uzhhorod National University, Pidhirna Str., 46, Uzhhorod 88000, Ukraine.
[2]Pavol Jozef Šafárik University in Košice, 041 54 Košice, Slovak Republic.
[3]Department of Condensed Matter Physics, Faculty of Mathematics and Physics, Charles University, Ke Karlovu 5, CZ-12116 Prague 2, Czech Republic.

References

1. Mitsa V, Holomb R, Veres M, Marton A, Rosola I, Fekeshgazi I, Koós M (2011) Non-linear optical properties and structure of wide band gap non-crystalline semiconductors. Phys Status Solidi C 9:2696–2670
2. Zeller R, Pohl R (1971) Thermal conductivity and specific heat of non-crystalline solids. Phys Rev B 4:2029–2041
3. Stephens R (1973) Low-temperature specific heat and thermal conductivity of non-crystalline dielectric solids. Phys Rev B 8:2029–2940
4. Leadbetter A, Jeapes C, Watereld R, Maynard R (1977) Conduction thermique des verres aux basses températures. Journal de Physique 38:95–99
5. Phillips W (1972) Tunnelling states in amorphous solids. J Low Temp Phys 7:351–360
6. Anderson PW, Halperin BI, Varma CM (1972) Anomalous low-temperature thermal properties of glasses and spin glasses. Phil Mag 25:1–9
7. Leggett AJ (1988) Low temperature properties of amorphous materials: through a glass darkly. Comments Cond Mat Phys 14:231–251
8. Bermann R (1976) Thermal conduction in solids. Clarendon Press, Oxford
9. Karpov VG, Parshin DA (1985) On the thermal conductivity of glasses at temperatures below the Debye temperature. Zh Eksp Teor Fiz (Russia) 88:2212–2227
10. Malinovsky V, Novikov V, Parshin P, Sokolov A, Zemlyanov M (1990) Universal form of the low-energy (2-10 meV) vibrational spectrum of glasses. Europhysics Letters 11:43–47
11. Sokolov A, Kisliuk A, Quitmann D, Duval E (1993) Evaluation of density of vibrational states of glasses from low-frequency Raman spectra. Phis Rev 48:7692–8002
12. Nakayama T, Orbach R (1999) On the increase of thermal conductivity in glasses above the plateau region. Physica B 263-264:261–263
13. Jagannathan A, Orbach R, Entin-Wohlman O (1989) Thermal conductivity of amorphous materials above the plateau. Phys Rev B 39:13465–1377
14. Feher A, Yurkin IM, Deich LI, Orendach M, Turyanitsa ID (1994) The comparative analysis of some low-frequency vibrational state density models of the amorphous materials—applied to the As_2S_3 glass. Physica B 194–196:395–396
15. Vateva E, Terziyska B, Arsova D (2007) Low-temperature specific heat and thermal conductivity of ternary chalcogenide glasses. J Optoel Adv Mat 9:1965–1973
16. Schrimacher W, Diezemann G, Ganter C (1998) Harmonic vibrational excitations in disordered solids and "boson peak". Phys Rev Lett 81:136–140
17. Feldman JL, Kluge MD, Allen PB, Wooten F (1993) Thermal conductivity and localization in glasses: numerical study of a model of amorphous silicon. Phys Rev B 48:12589
18. Denisov YV, Zubovich AA (2003) The role of vibrations of medium-range order clusters in thermal conduction of materials with a disordered structure glass. J Physics and Chemistry 29:237–242
19. Kedar S, Abhay KS, Saxena NS (2008) Temperature dependence of effective thermal conductivity and effective thermal diffusivity of $Se_{90}In_{10}$ bulk chalcogenide glass. Current Applied Physics 8:159–164
20. Holomb R, Mitsa V (2004) Boson peak of As_xS_{100-x} glasses and theoretical calculations of low frequencies clusters vibrations. Solid State Commun 129:655–2004
21. Holomb R, Mitsa V, Johansson P, Veres M (2010) Boson peak in low-frequency Raman spectra of As_xS_{100-x} glasses: nanocluster contribution. Phys Status Sol C 7:885–888
22. Jakse N, Nassour A, Pasturel A (2012) Structural and dynamic origin of the boson peak in a Cu-Zr metallic glass Phys. Rev B 85:174201
23. Holomb R, Veres M, Mitsa V (2009) Ring-, branchy-, and cage-like As_nS_m nanoclusters in the structure of amorphous semiconductors: *ab initio* and Raman study. J Optoel Adv Mat 11:917–923
24. Holomb RM, Mitsa VM (2004) Simulation of Raman spectra of As_xS_{100-x} glasses by the results of ab initio calculations of As_nS_m clusters vibrations. J Optoel Adv Mat 6:1177–1184
25. Holomb R, Mateleshko N, Mitsa V, Johansson P, Matic A, Veres M (2006) New evidence of light-induced structural changes detected in As-S glasses by photon energy dependent Raman spectroscopy. J Non-Cryst Sol 352:1607–1611
26. Schmidt MW, Baldridge KK, Boatz JA, Elbert ST, Gordon MS, Jensen JJ, Koseki S, Matsunaga N, Nguyen KA, Su S, Windus TL, Dupuis M, Montgomery JA (1993) General atomic and molecular electronic structure system. J Combz Chem 14:1347–1363
27. Becke AD (1988) Density-functional exchange-energy approximation with correct asymptotic behavior. Phys Rev A 38:3098–3100
28. Lee C, Yang W, Parr RG (1988) Development of the Colle-Salvetti correlation-energy formula into a functional of the electron density. Phys Rev B 37:785–789
29. EMSL Basis Set Library (https://bse.pnl.gov/bse/portal)
30. Billes F, Mitsa V, Fejes I, Mateleshko N, Fejsa I (1999) Calculation of the vibrational spectra of arsenic sulfide clusters. J Molec Struct 513:109–115